The EMBO Journal vol.13 no.11 pp.2708–2713, 1994

Yeast Kar3 is a minus-end microtubule motor protein that destabilizes microtubules preferentially at the minus ends

Sharyn A.Endow, Sang J.Kang, Lisa L.Satterwhite[1], Mark D.Rose[1], Victoria P.Skeen[2] and E.D.Salmon[2]

Department of Microbiology, Duke University Medical Center, Durham, NC 27710, [1]Department of Biology, Princeton University, Princeton, NJ 08544 and [2]Department of Biology, University of North Carolina, Chapel Hill, NC 27599, USA

Communicated by T.Kreis

Mutants of the yeast Kar3 protein are defective in nuclear fusion, or karyogamy, during mating and show slow mitotic growth, indicating a requirement for the protein both during mating and in mitosis. DNA sequence analysis predicts that Kar3 is a microtubule motor protein related to kinesin, but with the motor domain at the C-terminus of the protein rather than the N-terminus as in kinesin heavy chain. We have expressed Kar3 as a fusion protein with glutathione *S*-transferase (GST) and determined the *in vitro* motility properties of the bacterially expressed protein. The GST–Kar3 fusion protein bound to a coverslip translocates microtubules in gliding assays with a velocity of 1–2 μm/min and moves towards microtubule minus ends, unlike kinesin but like kinesin-related *Drosophila* ncd. Taxol-stabilized microtubules bound to GST–Kar3 on a coverslip shorten as they glide, resulting in faster lagging end, than leading end, velocities. Comparison of lagging and leading end velocities with velocities of asymmetrical axoneme–microtubule complexes indicates that microtubules shorten preferentially from the lagging or minus ends. The minus end-directed translocation and microtubule bundling of GST–Kar3 is consistent with models in which the Kar3 protein crosslinks internuclear microtubules and mediates nuclear fusion by moving towards microtubule minus ends, pulling the two nuclei together. In mitotic cells, the minus end motility of Kar3 could move chromosomes polewards, either by attaching to kinetochores and moving them polewards along microtubules, or by attaching to kinetochore microtubules and pulling them polewards along other polar microtubules. The destabilization at microtubule minus ends observed in our *in vitro* studies suggests that Kar3 may also function to promote microtubule depolymerization at spindle pole bodies during karyogamy and mitosis. The minus end polarity of Kar3 and ncd translocation, and the structural similarity to Kar3 and ncd of kinesin-related proteins from *Arabidopsis* and mammalian cells, support the idea that a unique subfamily of the kinesin proteins consists of minus end-directed motors.

Key words: karyogamy/microtubule depolymerization/microtubule motor protein/mitosis

Introduction

A *kar3* mutant was first identified in a screen for mutants defective in nuclear fusion, or karyogamy, during mating (Polaina and Conde, 1982). Characterization of *kar3* disruption mutants showed a phenotype of slow mitotic growth in addition to a severe defect in karyogamy (Meluh and Rose, 1990). *kar3* disruption mutant zygotes typically exhibited two separated nuclei associated with long cytoplasmic microtubules that failed to interdigitate with one another, in contrast to the single fused nucleus of wild-type zygotes. Furthermore, mitotically growing cultures of *kar3* mutant cells accumulated large budded cells with a single nucleus and a short mitotic spindle, characteristic of cell cycle arrest in mitosis. Immunolocalization of Kar3 using a β-galactosidase–Kar3 fusion protein showed microtubule-dependent localization to spindle pole bodies, co-localization with cytoplasmic microtubules (Meluh and Rose, 1990) and localization to the mitotic apparatus (Page *et al.*, 1994).

DNA sequence analysis of *KAR3* (Meluh and Rose, 1990) predicts that the Kar3 protein is a microtubule motor protein related to the mechanochemical protein, kinesin. Kinesin binds to microtubules and translocates on microtubules in the presence of ATP, transporting bound subcellular components. Kinesin is implicated in vesicle and organelle transport in neuronal cells and is thought to be the basis of fast axonal transport. In *in vitro* motility assays, kinesin moves towards the fast polymerizing/depolymerizing microtubule plus ends. The predicted Kar3 protein contains a region similar to the ATP- and microtubule-binding 'motor' domain of kinesin heavy chain, and a bacterially expressed Kar3 protein shows microtubule-stimulated ATPase activity *in vitro* (Meluh, 1992). The position of the motor region in the Kar3 protein differs from that of kinesin heavy chain, however, in that it is located at the C-terminus of the protein rather than the N-terminus as in kinesin heavy chain (Meluh and Rose, 1990). Another kinesin-related protein with a C-terminal motor domain, *Drosophila* ncd, has been demonstrated to be a microtubule motor protein that moves with the opposite polarity to kinesin, towards microtubule minus ends (McDonald *et al.*, 1990; Walker *et al.*, 1990). Outside of the motor domain, Kar3 differs in amino acid sequence from kinesin heavy chain and also from ncd, although the non-motor 'tail' region of Kar3 resembles that of ncd in that this region of both proteins is basic (calculated pI ~12) and proline-rich (8–10%). The dissimilarity of the Kar3 non-motor region to the non-motor region of kinesin heavy chain and its similarity to ncd suggest that Kar3 and ncd perform related functions in the cell that differ from that of kinesin.

The role of Kar3 in mitosis has been investigated by constructing cells deficient in Kar3 and two other kinesin-related proteins, Cin8 and Kip1, implicated in spindle

assembly in yeast (Saunders and Hoyt, 1992). Cells mutant for all three kinesin proteins showed a less severe phenotype of spindle collapse than the *cin8/kip1* double mutant. The partial suppression of the double mutant phenotype by a *kar3* deletion was interpreted to mean that Kar3 contributes to spindle assembly by opposing forces generated by Cin8 and Kip1 in separating spindle poles prior to anaphase (Saunders and Hoyt, 1992).

Determination of the role of Kar3 in karyogamy and mitosis is dependent on information regarding the motility properties of the protein. In particular, models for Kar3 function require knowledge of the polarity of Kar3 movement on microtubules and other properties of the motor. We have therefore expressed Kar3 as a glutathione *S*-transferase (GST) fusion protein and assayed the GST−Kar3 fusion protein in *in vitro* motility assays. We find that bacterially expressed GST−Kar3 is a microtubule motor that translocates towards the minus end of microtubules, like *Drosophila* ncd (McDonald *et al.*, 1990; Walker *et al.*, 1990) but unlike plus end-directed kinesin. The GST−Kar3 motor protein supports microtubule translocation at ~1−2 μm/min and causes extensive bundling of microtubules in motility assays. An unusual property of GST−Kar3 is the ability of the protein to destabilize taxol-stabilized microtubules, preferentially at their minus ends.

Results

Bacterially expressed Kar3 is a microtubule motor protein

Kar3 protein was expressed in bacterial cells as a GST fusion protein (Smith and Johnson, 1988) containing 108 residues of the predicted 275 residue α-helical coiled coil central region together with the entire C-terminal motor domain (Figure 1). The GST−Kar3 fusion protein is missing residues 1−276, corresponding to the tail and part of the stalk of the predicted wild-type Kar3 protein, but contains an intact motor domain. Similar truncated kinesin proteins fused to GST have been demonstrated to translocate on microtubules with the same polarity and velocity as the native protein or near full-length expressed proteins (Chandra *et al.*, 1993; Stewart *et al.*, 1993).

Bacterial lysates enriched in the induced GST−Kar3 protein were prepared (Chandra and Endow, 1993) and used in *in vitro* motility assays (Walker *et al.*, 1990; Chandra *et al.*, 1993). For some experiments, GST−Kar3 protein was purified using S-Sepharose chromatography (Figure 2). Microtubules were assembled from purified mammalian brain tubulin and assays were carried out in the presence of 5 mM MgATP, unless otherwise indicated.

In solution, GST−Kar3 caused extensive bundling of taxol-stabilized microtubules as assayed using video-enhanced differential interference contrast (VE-DIC) microscopy (Walker *et al.*, 1988). When adsorbed to coverslips coated with anti-GST antibody, and in the presence of 0.5× salt solution and 5 mM MgATP, GST−Kar3 bound taxol-stabilized microtubules to the glass surface and supported microtubule gliding at velocities of 1−2 μm/min (Figure 3), demonstrating that the bacterially expressed fusion protein is a microtubule motor protein. Microtubules were efficiently bound to the coverslip surface by GST−Kar3 and most of the unbundled, single microtubules showed movement.

GST−Kar3 translocates towards microtubule minus ends

The polarity of GST−Kar3 movement on microtubules was determined using asymmetrical axoneme−microtubule complexes prepared by growing microtubules from the plus ends of axoneme fragments (Vale and Toyoshima, 1988; Walker *et al.*, 1990; Hyman *et al.*, 1991). The axoneme−microtubule complexes translocated on GST−Kar3 protein adsorbed to anti-GST antibody-coated coverslips with the microtubule (plus) end leading (Figure 3). Because the GST−Kar3 protein was bound to the glass surface, this result showed that GST−Kar3 protein moves along the microtubule lattice towards the minus end. Twenty-six clearly labelled axoneme−microtubule complexes all translocated with the microtubule end leading. As a control, axoneme−microtubule complexes bound to conventional neuronal kinesin were observed and all were found to translocate with the axoneme end leading (n = 35), consistent with the plus end polarity of kinesin movement (Vale *et al.*, 1985). The velocity of axoneme−microtubule movement on GST−Kar3 was determined by tracking complexes at the junction between the axoneme and microtubule, and found to be 1.2 ± 0.4 μm/min (x ± SD, n = 11).

GST−Kar3 preferentially destabilizes gliding microtubules at the minus ends

Surprisingly, taxol-stabilized single microtubules (not complexed to axonemes) in assays of induced GST−Kar3 lysates containing 3.6 μM tubulin dimer and 0.71 μM taxol showed shortening preferentially at the minus ends, as

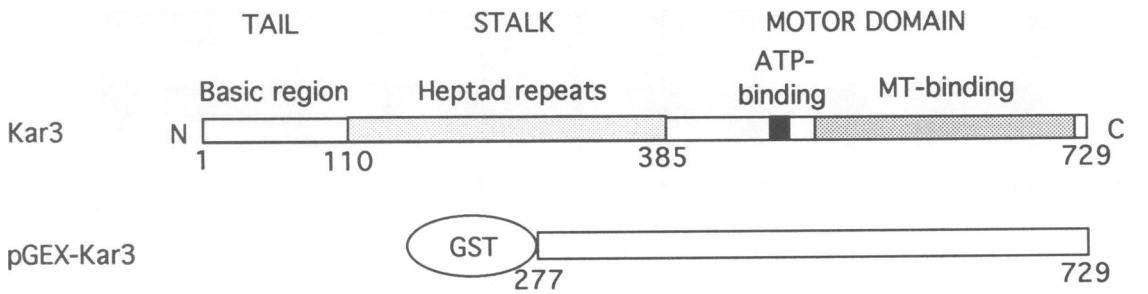

Fig. 1. Expression of Kar3 as a GST−Kar3 fusion protein. The predicted Kar3 protein is 729 amino acids in length and has the putative motor domain (residues 385−729) at the C-terminus of the protein (Meluh and Rose, 1990). The 26 kDa GST protein is present at the N-terminus of the GST−Kar3 fusion protein. The GST−Kar3 fusion protein contains residues 277−729 of the predicted Kar3 protein, corresponding to part of the central coiled coil region and the entire C-terminal motor domain.

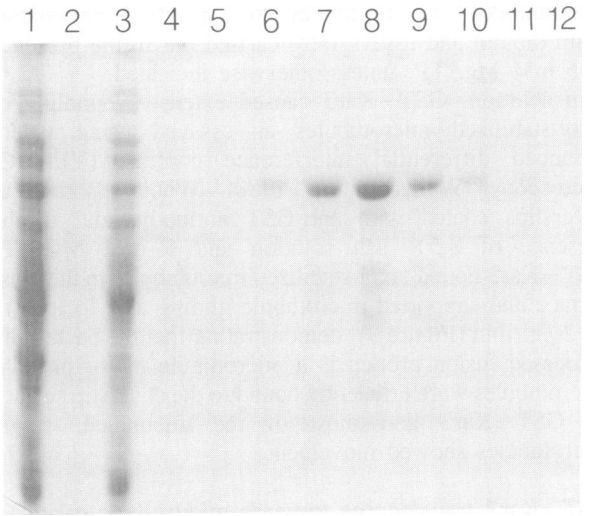

Fig. 2. Purification of bacterially expressed GST−Kar3 by chromatography on S-Sepharose. Column fractions were analyzed by SDS−PAGE. Lane 1, column load; lane 2, breakthrough; lane 3, PB wash; lane 4, PB + 40 mM NaCl wash; lane 5, PB + 100 mM NaCl wash; lanes 6−12, step elution with PB + 200 mM NaCl. The peak fraction (lane 8) was dialyzed against PB + 0.5 mM DTT + 0.5 mM PMSF for 90 min and used in motility assays. The GST−Kar3 protein has a predicted M_r of ~78 kDa and cross-reacts with anti-HIPYR antibody (Sawin *et al.*, 1992), directed against a conserved sequence motif in the kinesin motor domain. The GST−Kar3 protein is estimated to be ~80−90% pure.

indicated by velocity measurements of leading and lagging microtubule ends (Figure 3), compared with the velocity of axoneme−microtubule complexes. The average velocity of the leading (plus) ends was 1.2 ± 0.5 μm/min (x ± SD, n = 10), similar to the value determined for the asymmetrical axoneme−microtubule complexes. The average velocity of the lagging (minus) ends was 1.8 ± 0.3 μm/min (x ± SD, n = 10). The difference in leading and lagging end velocities was attributed to preferential depolymerization of microtubules at minus ends, based on the similarity in leading end velocity to the velocity of the axoneme−microtubule complexes. Depolymerization was also observed at the leading (plus) ends of axoneme−microtubule complexes gliding on Kar3 lysates, but the rate of shortening was much slower than found for minus ends of single non-complexed microtubules. The rate of plus end shortening was estimated to be ~0.15 μm/min or less, based on measurement of the microtubule region of one axoneme−microtubule complex after 5.9 min.

Shortening of microtubules was also observed for S-Sepharose-purified GST−Kar3 in motility assays containing 1.8 μM tubulin dimer and 0.36 or 0.71 μM taxol, and 5 mM MgATP or 5 mM MgGTP (Table I). The frequency of microtubules that shortened preferentially from one end in assays containing GST−Kar3 and 5 mM MgATP was >75% (n = 113/144 in one set of experiments) and the average velocity of shortening was ~0.4 μm/min, as calculated from the difference in leading and lagging end

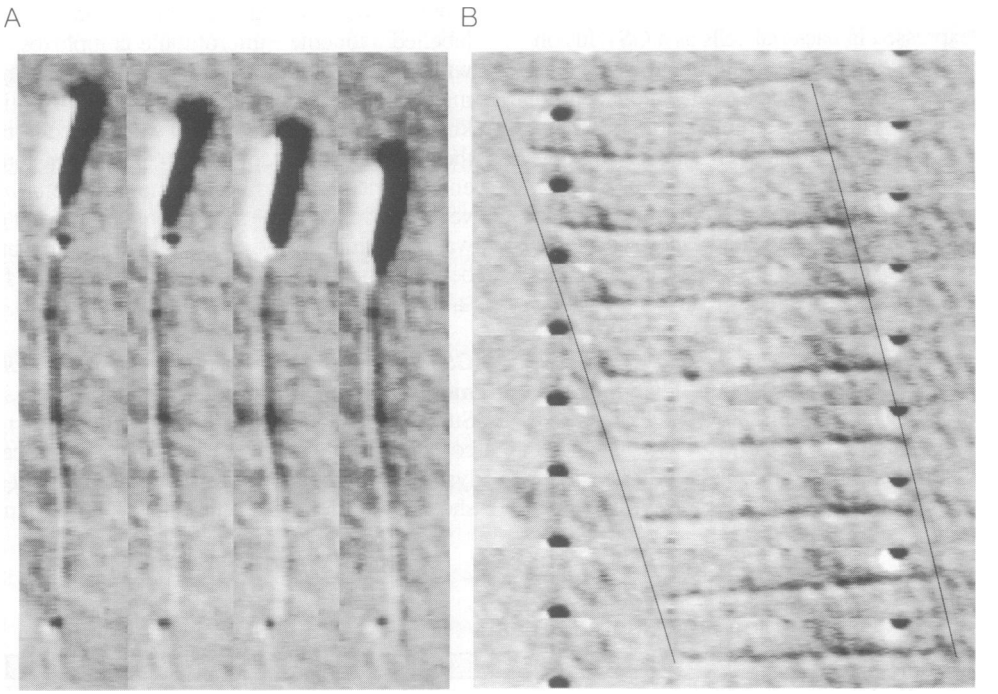

Fig. 3. Polarity of movement on microtubules and microtubule shortening induced by GST−Kar3. (**A**) Polarity of GST−Kar3 movement on microtubules, assayed using asymmetrical axoneme−microtubule complexes. Images taken at 20 s intervals over a 60 s period are shown (left to right). Two stationary particles are shown for orientation. The time lapse series shows that the microtubule (plus) end of the complex is leading, indicating that the GST−Kar3 motor protein is moving towards the microtubule minus end. This identifies the leading end of the microtubule shown in (**B**) as the plus end and the lagging end as the minus end. (**B**) A taxol-stabilized microtubule translocating on GST−Kar3 bound to a coverslip shortens as it moves. Images taken at 20 s intervals are shown over a 160 s period (top to bottom). Two stationary particles are shown for orientation. The slopes of lines drawn through the microtubule ends at each time point indicate the relative velocities of leading (1.3 μm/min) and lagging (1.6 μm/min) ends. Depolymerization is faster at the lagging (minus) end than at the leading (plus) end, as reflected in the faster velocity of lagging end microtubule movement. The 8.1 μm microtubule has shortened ~0.7 μm in the time sequence shown.

Table I. Nucleotide dependence of microtubule gliding and shortening produced by GST−Kar3

GST−Kar3	Nucleotide	MT gliding		MT shortening (one end)	
		Relative number	Leading end velocity[a]	Relative number	Estimated velocity[a]
+	5 mM MgATP	>60−70%	1.3 ± 0.1	>75%	~0.4
+	5 mM MgGTP	~30−35%	0.4 ± 0.1	~70%	~0.3
+	5 mM MgAMP·PNP	−	0	~15%[b]	ND
−	5 mM MgATP	−	0	<10%	~0.17

MT = microtubule, ND = not determined.
[a]Units are μm/min.
[b]One experiment only, 2/13 microtubules shortened from one end within 2−3 min observation.
Percentages indicate the relative numbers of microtubules monitored that showed gliding or shortening in motility assays with or without GST−Kar3 and the indicated nucleotide. In assays without GST−Kar3, PB buffer (see Materials and methods) was substituted for the GST−Kar3. Microtubules stick to the anti-GST antibody coating on the coverslip in the absence of the Kar3 motor protein under the conditions of our assay. Motility experiments were performed using S-Sepharose-purified GST−Kar3 protein. Final tubulin dimer concentration was 1.8 μM and final taxol concentration was 0.71 or 0.36 μM. Increasing the final taxol concentration to 3.9 μM fully stabilized microtubules bound to coverslips in the absence of GST−Kar3, and inhibited but did not prevent shortening of microtubules bound to GST−Kar3. Estimates for velocities of microtubule shortening in the presence of GST−Kar3 were made by subtracting leading end from lagging end velocities of gliding microtubules. The velocity of shortening for the few microtubules that showed instability in the absence of GST−Kar3 was determined from measurements made directly on the video monitor.

velocities of microtubules gliding on S-Sepharose-purified GST−Kar3 (see below).

Control slides of microtubules bound to anti-GST antibody on a coverslip in assays containing 1.8 μM tubulin dimer, 0.36 or 0.71 μM taxol, 5 mM MgATP and 0.5× salts, but no GST−Kar3 motor protein, showed shortening of <10% of bound microtubules (n = 9/120) (Table I). The estimated rate of depolymerization for the few unstable microtubules in the control slides was ~0.17 μm/min. These data demonstrate that the taxol-stabilized microtubules that we used in our assays were relatively stable in the absence of the GST−Kar3 protein.

Increasing the taxol concentration in the control experiments by ~5- to 10-fold to 3.9 μM fully stabilized microtubules bound to the coverslip in the absence of GST−Kar3 (n = 24/24). The higher taxol concentration inhibited microtubule shortening in the presence of GST−Kar3, but did not prevent it: >40% of microtubules (n = 36/88) bound to GST−Kar3 in higher taxol shortened preferentially from one end. Both stationary and gliding microtubules shortened from one end, and the lagging ends showed a greater displacement than the leading end for gliding microtubules. These, plus the above, data demonstrate that microtubules bound to GST−Kar3 on a coverslip in the presence of added nucleotide showed greatly enhanced instability at their lagging ends, identified as the minus ends from our polarity experiments.

Nucleotide dependence of microtubule gliding on GST−Kar3

S-Sepharose-purified GST−Kar3 was used to assay nucleotide dependence of microtubule gliding and shortening. Microtubules showed extensive bundling and clumping by S-Sepharose-purified GST−Kar3 protein. In the presence of 5 mM MgATP, single microtubules glided with leading end (1.3 ± 0.1 μm/min) (x ± SD, n = 18) and lagging end (1.7 ± 0.2 μm/min) (x ± SD, n = 18) velocities similar to those of microtubules moving on lysates of GST−Kar3 in 5 mM MgATP. More than 60−70% of single microtubules bound to S-Sepharose-purified GST−Kar3 glided in the presence of 5 mM MgATP. Microtubule movement was greatly reduced in 5 mM MgGTP compared with 5 mM MgATP, but slow translocation was observed for ~30−35% of single microtubules that were monitored. Measurement of gliding microtubules in 5 mM MgGTP resulted in velocities of 0.4 ± 0.1 μm/min (x ± SD, n = 19) for the leading end and 0.7 ± 0.1 μm/min (x ± SD, n = 19) for the lagging end (Table I). Thus, utilization of MgGTP by GST−Kar3 was relatively inefficient compared with MgATP. No movement and infrequent (n = 2/13) shortening of microtubules was observed in 5 mM MgAMP·PNP, a non-hydrolyzable ATP analog (Table I).

Discussion

Kar3 is a minus end-directed microtubule motor protein

Our findings show that Kar3 is a 'slow' (1−2 μm/min) minus end-directed microtubule motor protein, in contrast to kinesin which is a 'fast' (30 μm/min) plus end-directed motor. The slow velocity of our bacterially expressed Kar3 motor may be related to a slower turnover of ATP (k_{cat} ~0.048 s^{-1}) [calculated from Meluh (1992)], relative to kinesin (k_{cat} ~6−9 s^{-1}) (Hackney, 1988; Sadhu and Taylor, 1992), in the presence of microtubules, as assayed using a similarly truncated bacterially expressed and partially purified Kar3 protein. The values reported for *Drosophila* ncd velocity (4−15 μm/min) (McDonald *et al.*, 1990; Walker *et al.*, 1990) and ATPase activity in the presence of microtubules (k_{cat} ~0.30−1.05 s^{-1}) (Chandra *et al.*, 1993; Lockhart and Cross, 1994) fall between those of Kar3 and kinesin, strengthening this correlation.

The minus end-directed polarity of Kar3 resolves a number of conflicting models of how Kar3 may be functioning in karyogamy and mitosis in yeast. Our results support models of Kar3 function in karyogamy in which Kar3 is proposed to crossbridge antiparallel microtubules that lie between the two haploid nuclei and pull the nuclei together by moving

towards microtubule minus ends (Meluh and Rose, 1990; Rose, 1991). Based on genetic studies, Kar3 has also been proposed (Saunders and Hoyt, 1992) to antagonize the action of two other kinesin-related proteins, Cin8 and Kip1, which are involved in pushing the spindle poles apart. Our finding that Kar3 is a minus end-directed motor substantially strengthens this argument.

The Kar3 motor may also contribute to polewards movement of chromosomes by acting as a kinetochore motor (Hyman and Mitchison, 1991; Hyman *et al.*, 1992) and/or by attaching to kinetochore microtubules and pulling them polewards (poleward flux) along other polar microtubules (Mitchison and Salmon, 1993). In particular, the minus end-directed polarity and slow velocity of Kar3 movement observed in our motility assays is similar to the motion along microtubules exhibited by isolated yeast centromere DNA–protein complexes in yeast cytoplasmic extracts (Hyman *et al.*, 1992).

Kar3 destabilizes microtubules preferentially at the minus ends

The shortening at the minus ends of taxol-stabilized microtubules that we observe for GST–Kar3 protein may be the result of Kar3 inhibition of taxol stabilization of microtubules under the conditions of our *in vitro* motility assays. Increasing the taxol concentration to a stoichiometry of 2 taxol:1 tubulin dimer reduces, but does not prevent, shortening of microtubules bound to GST–Kar3. Destabilization of microtubules in our assays could be caused by GST–Kar3 bound to the coverslip or present in solution. There is also evidence that Kar3 is involved in regulating microtubule assembly in yeast. Mating *kar3* mutants have abnormally long cytoplasmic microtubules (Meluh and Rose, 1990; Vallen *et al.*, 1992) and it has been proposed that Kar3 is important in shortening microtubules between the nuclei as they move towards one another. In addition, low levels of the microtubule destabilizing drug, benomyl, can suppress the mitotic defect of *kar3* mutants (Roof *et al.*, 1991). A β-galactosidase–Kar3 fusion protein has been localized to the spindle pole body as well as cytoplasmic microtubules (Meluh and Rose, 1990), so that it is possible that Kar3 acts at the spindle pole bodies to promote minus end depolymerization as microtubules flux polewards during both karyogamy and mitosis. The basis of poleward microtubule flux has not yet been determined, but is thought to involve both microtubule dynamics and microtubule motors (Mitchison and Salmon, 1992).

Kar3 is a member of a unique subfamily of kinesin motor proteins

Kar3 is the second kinesin protein reported to date that translocates towards microtubule minus ends. *Drosophila* ncd was found previously to be a minus end microtubule motor protein (McDonald *et al.*, 1990; Walker *et al.*, 1990). Like ncd, the motor domain of Kar3 is at the C-terminus of the protein, rather than the N-terminus as in kinesin heavy chain and most of the other kinesin-related proteins identified to date. In addition to Kar3 and ncd, predicted kinesin proteins with C-terminal motor domains have been found in *Arabidopsis* (Mitsui *et al.*, 1993) and Chinese hamster ovary cells (Dragas-Granoic *et al.*, 1993; Wordeman and Mitchison, 1993), as well as other fungi (O'Connell *et al.*, 1993; Pidoux and Cande, 1993; Troxell and McIntosh, 1993). This broad distribution among widely divergent organisms suggests that these proteins are likely to be present in most or all eukaryotes, forming a subfamily of the kinesin-related proteins (Goodson *et al.*, 1994). The finding that two divergent members of the C-terminal motor kinesin proteins, Kar3 and ncd, are minus end microtubule motors indicates that other members of this unique kinesin subfamily are also likely to be minus end-directed microtubule motors. In mitotic vertebrate cells, the polewards movement of kinetochores over kinetochore microtubules (Skibbens *et al.*, 1993) has the directionality and velocity to be driven by microtubule motors like Kar3 and ncd.

Materials and methods

Construction of the GST–KAR3 plasmid

A plasmid for expression of Kar3 as a fusion protein with GST was constructed by ligating an *Nde*I-digested and repaired DNA fragment encoding residues 277–729 of the predicted Kar3 protein to *Sma*I-digested pGEX-2T plasmid (Smith and Johnson, 1988). The GST–Kar3 fusion protein has GST at the N-terminus and contains 108 residues of the 275 residue central heptad repeat region of the predicted Kar3 protein, together with the entire C-terminal motor domain. A non-fusion protein corresponding to the same region of Kar3 has been demonstrated to be a microtubule-stimulated ATPase *in vitro* (Meluh, 1992).

Expression and purification of GST–Kar3

The GST–Kar3 plasmid was transformed into BL21(DE3)pLysS host cells (Studier *et al.*, 1990) for expression in bacteria. Cells were grown at 37°C to A_{550} = 0.6–1.0, rapidly cooled to 22°C, IPTG was added to 0.4 mM and protein was induced by growth at 22°C for 1 h. Induced cells were pelleted and stored at −70°C. Lysates were prepared as described previously (Chandra and Endow, 1993). Briefly, cells were lysed by freeze–thawing in PB (10 mM $NaPO_4$, pH 7.4, 1 mM EGTA, 1 mM $MgCl_2$) plus protease inhibitors, treated with DNase I to digest bacterial DNA, and centrifuged at 27 000 *g* for 30 min at 4°C to pellet cell debris. The supernatant was recentrifuged at 15 600 *g* for 15 min and then at 196 000 *g* for 30 min. The final supernatant was used in *in vitro* motility assays.

S-Sepharose-purified protein was prepared by passing the 15 600 *g* supernatant over a 1 ml column of S-Sepharose in PB. The GST–Kar3 protein binds to S-Sepharose and elutes at 0.2 M NaCl. Excess NaCl was removed by dialysis in PB containing 0.5 mM DTT and 0.5 mM phenylmethylsulfonyl fluoride (PMSF) for 90 min and the dialyzed protein was used in motility assays. The S-Sepharose-purified GST–Kar3 protein was estimated to be ~80–90% pure by SDS–PAGE.

In vitro motility assays

Motility assays of induced GST–Kar3 protein lysates were carried out at 22°C essentially as described (Walker *et al.*, 1990; Chandra *et al.*, 1993). Coverslips were coated with 7 μl affinity-purified anti-GST antibody (A_{280} = 0.5), protein was allowed to adsorb for 1 min at 22°C, and excess antibody was removed by rinsing twice with 30 μl PEM (100 mM PIPES, pH 6.9, 2 mM EGTA, 1 mM $MgSO_4$) or, in some experiments, PB. After draining, 5 μl GST–Kar3 were applied to the coverslip together with 1.6 μl taxol-stabilized microtubules (final tubulin dimer concentration = 3.6 μM; final taxol concentration = 0.71 μM) or axoneme–microtubule complexes, 6× salt solution (final concentration = 0.5×; 6× = 70 mM PIPES, pH 6.9, 480 mM NaCl, 30 mM $MgCl_2$, 0.7 mM $MgSO_4$, 1.4 mM EGTA, 4.8 mM DTT) and MgATP (final concentration = 5 mM). The final volume was 9 μl. In experiments with S-Sepharose-purified GST–Kar3 protein, the final tubulin dimer concentration was 1.8 μM and the final taxol concentration was 0.36 or 0.71 μM. In higher taxol experiments, the final tubulin dimer and taxol concentrations were 1.8 and 3.9 μM, respectively.

Motility was recorded using VE-DIC microscopy (Walker *et al.*, 1988). Velocities of microtubule ends were measured by tracking microtubules using a mouse-driven video cursor overlaid on images played back from a video tape, as described previously (Walker *et al.*, 1988). Home-written software was used to display the cursor position with time and to calculate standard regression curves through the data points. Velocities were determined by

averaging two to four determinations for each microtubule end. Microtubule ends were typically tracked for ~2 min for each determination. Kinetographs of microtubule movement were made from video recordings using a Metamorph digital processing system (Universal Imaging Corp., West Chester, PA).

Assays carried out without precoating coverslips with anti-GST antibody resulted in reduced motility, and assays without 0.5× salt solution resulted in extensive bundling of microtubules. Axoneme–microtubule complexes were prepared by assembling microtubules selectively onto the plus ends of sea urchin axoneme fragments, as described previously (Vale and Toyoshima, 1988; Walker *et al.*, 1990; Hyman *et al.*, 1991). Microtubules were assembled onto axoneme fragments in 20 μl reaction mixtures containing equimolar tubulin and *N*-ethyl maleimide-modified tubulin (final tubulin dimer concentration = 16 μM each) for 10–30 min at 37°C. The resulting asymmetrical complexes were diluted 5-fold into PEM buffer containing taxol (final taxol concentration = 4 μM) and used in the coverslip gliding assay.

Acknowledgements

R.Mandell contributed to the construction of the pGEX-Kar3 plasmid used in these studies. We thank R.A.Walker for the generous gift of chicken brain kinesin, and K.Bloom and E.Yeh for comments on the manuscript. S.A.Endow thanks N.Teichmann of Carl Zeiss, Inc. for assistance in setting up a video microscope. This research was supported by USPHS and ACS grants to S.A.Endow, and USPHS grants to M.D.Rose and E.D.Salmon. L.L.Satterwhite is the recipient of a Damon Runyun-Walter Winchell Cancer Research Fund postdoctoral fellowship.

References

Chandra,R. and Endow,S.A. (1993) *Methods Cell Biol.*, **39**, 115–127.
Chandra,R., Salmon,E.D., Erickson,H.P., Lockhart,A. and Endow,S.A. (1993) *J. Biol. Chem.*, **268**, 9005–9013.
Dragas-Granoic,S., Kato,T., Khodjakov,A., Kofron,M. and Kuriyama,R. (1993) *Mol. Biol. Cell*, **4**, 243.
Goodson,H.V., Kang,S.J. and Endow,S.A. (1994) *J. Cell Sci.*, in press.
Hackney,D.D. (1988) *Proc. Natl Acad. Sci. USA*, **85**, 6314–6318.
Hyman,A.A. and Mitchison,T.J. (1991) *Nature*, **351**, 206–211.
Hyman,A., Drechsel,D., Kellogg,D., Salser,S., Sawin,K., Steffen,P., Wordeman,L. and Mitchison,T. (1991) *Methods Enzymol.*, **196**, 478–485.
Hyman,A.A., Middleton,K., Centola,M., Mitchison,T.J. and Carbon,J. (1992) *Nature*, **359**, 533–536.
Lockhart,A. and Cross,R.A. (1994) *EMBO J.*, **13**, 751–757.
McDonald,H.B., Stewart,R.J. and Goldstein,L.S.B. (1990) *Cell*, **63**, 1159–1165.
Meluh,P.B. (1992) *Kar3, A Kinesin-Related Gene Required for Nuclear Fusion, Mitosis and Meiosis in Saccharomyces cerevisiae*. Princeton University, NJ.
Meluh,P.B. and Rose,M.D. (1990) *Cell*, **60**, 1029–1041.
Mitchison,T.J. and Salmon,E.D. (1992) *J. Cell Biol.*, **119**, 569–582.
Mitsui,H., Yamaguchi-Shinozaki,K., Shinozaki,K., Nishikawa,K. and Takahashi,H. (1993) *Mol. Gen. Genet.*, **238**, 362–368.
O'Connell,M.J., Meluh,P.B., Rose,M.D. and Morris,N.R. (1993) *J. Cell Biol.*, **120**, 153–162.
Page,B.D., Satterwhite,L.L., Rose,M.D. and Snyder,M. (1994) *J. Cell Biol.*, **124**, 507–519.
Pidoux,A.L. and Cande,W.Z. (1993) *Mol. Biol. Cell*, **4**, 243.
Polaina,J. and Conde,J. (1982) *Mol. Gen. Genet.*, **186**, 253–258.
Roof,D.M., Meluh,P.B. and Rose,M.D. (1991) *Cold Spring Harbor Symp. Quant. Biol.*, **55**, 693–703.
Rose,M.D. (1991) *Annu. Rev. Microbiol.*, **45**, 539–567.
Sadhu,A. and Taylor,E.W. (1992) *J. Biol. Chem.*, **267**, 11352–11359.
Saunders,W.S. and Hoyt,M.A. (1992) *Cell*, **70**, 451–458.
Sawin,K.E., Mitchison,T.J. and Wordeman,L.G. (1992) *J. Cell Sci.*, **101**, 303–313.
Skibbens,R.V., Skeen,V.P. and Salmon,E.D. (1993) *J. Cell Biol.*, **122**, 859–875.
Smith,D.B. and Johnson,K.S. (1988) *Gene*, **67**, 31–40.
Stewart,R.J., Thaler,J.P. and Goldstein,L.S.B. (1993) *Proc. Natl Acad. Sci. USA*, **90**, 5209–5213.
Studier,F.W., Rosenberg,A.H., Dunn,J.J. and Dubendorff,J.W. (1990) *Methods Enzymol.*, **185**, 60–89.
Troxell,C.L. and McIntosh,J.R. (1993) *Mol. Biol. Cell*, **4**, 243.
Vale,R.D. and Toyoshima,Y.Y. (1988) *Cell*, **52**, 459–469.
Vale,R.D., Schnapp,B.J., Mitchison,T., Steuer,E., Reese,T.S. and Sheetz,M.P. (1985) *Cell*, **43**, 623–632.
Vallen,E.A., Hiller,M.A., Scherson,T.Y. and Rose,M.D. (1992) *J. Cell Biol.*, **117**, 1277–1287.
Walker,R.A., O'Brien,E.T., Pryer,N.K., Soboeiro,M.F., Voter,W.A., Erickson,H.P. and Salmon,E.D. (1988) *J. Cell Biol.*, **107**, 1437–1448.
Walker,R.A., Salmon,E.D. and Endow,S.A. (1990) *Nature*, **347**, 780–782.
Wordeman,L. and Mitchison,T.J. (1993) *Mol. Biol. Cell*, **4**, 118.

Received on February 7, 1994; revised on March 22, 1994